



Research papers

Bio-optical characteristics along the Straits of Magallanes



Vivian Lutz^{a,b,*}, Robert Frouin^c, Rubén Negri^b, Ricardo Silva^b, Mayza Pompeu^d,
Natalia Rudorff^e, Anderson Cabral^f, Ana Dogliotti^g, Gustavo Martinez^h

^a IIMyC, CONICET, Mar del Plata, Argentina

^b INIDEP, Mar del Plata, Argentina

^c SIO - UCSD, La Jolla, USA

^d IO-USP, São Paulo, Brazil

^e INPE/CPTEC, Cachoeira Paulista, São Paulo, Brazil

^f IB/UFRJ, Rio de Janeiro, RJ, Brazil

^g IAFE, CONICET/UBA, Buenos Aires, Argentina

^h Subsecretaría de Pesca y Acuicultura – MAGyP, Buenos Aires, Argentina

ARTICLE INFO

Article history:

Received 30 September 2015

Received in revised form

2 March 2016

Accepted 8 March 2016

Available online 9 March 2016

Keywords:

Particulate absorption

CDOM absorption

Phytoplankton pigments

Carbon to chlorophyll ratio

Photoacclimation

Straits of Magallanes

ABSTRACT

The Straits of Magallanes at the tip of South America connects the Atlantic and Pacific Oceans. The variability in the absorption characteristics by phytoplankton ($a_{ph}(440)$), non-pigmented particles, NPP ($a_{NPP}(440)$), and chromophoric dissolved organic matter, CDOM ($a_y(440)$), measured along the Straits in late summer 2011 (R/V Melville MV1102 cruise), was analyzed. Satellite-derived monthly PAR data showed that at the time of the cruise the western sector was exposed to a low-light environment ($\sim 16 \text{ mol quanta m}^{-2}\text{d}^{-1}$) while the eastern sector received higher irradiance ($\sim 28 \text{ mol quanta m}^{-2}\text{d}^{-1}$). In the Patagonian Shelf total absorption was dominated by phytoplankton (up to 76%; $a_{ph}(440)=0.265 \text{ m}^{-1}$), while in the Atlantic Sector of the Straits, the major contributor was NPP (up to 42%; $a_{NPP}(440)=0.138 \text{ m}^{-1}$), and in the Pacific Sector of the Straits CDOM contributed up to 80% of the total absorption ($a_y(440)=0.232 \text{ m}^{-1}$). These changes could be related in part to the input of fresh water from glacier melting and rain in the Pacific Sector ($a_y(440)$ vs salinity $r_s = -0.98$). The carbon biomass (C) was composed in its majority by pico-phytoplankton and secondly by nano-phytoplankton, with exception of the Atlantic Sector where the micro-phytoplankton dominated. Carbon to chlorophyll-a ratios (C:Chla) were very low throughout the Straits (average of ~ 6) because of photoacclimation to the extremely low light. Complementary pigments data obtained in spring 2003 by the BEAGLE expedition indicated the predominance of diatoms all along the Straits, but the bio-optical trend resembled the one found in late summer 2011, i.e., NPP dominated the absorption in the well mixed Atlantic Sector, phytoplankton in the Middle Sector, and CDOM in the Pacific Sector. These results emphasize that underwater light is the major factor affecting phytoplankton growth and physiology, and that prevalent physical and geochemical conditions play an important role regulating the bio-optical properties in this heterogeneous area. These effects should be considered to adjust parameters (such as C:Chla) when running biogeochemical models for this region.

© 2016 Elsevier Ltd. All rights reserved.

1. Introduction

The underwater light field is one of the most important factors regulating life in the ocean. To start, phytoplankton needs light to

synthesize organic matter fueling the whole marine trophic web. Furthermore, the distribution of most organisms (including fishery resources) is conditioned by the transparency of the water either to favor grazing or predation, or to avoid it, at different stages of their life cycle. The intensity and spectral quality of light at sea is a function of the incident irradiance and the concentration and type of constituents present in the different regions and depths. These constituents, apart from water molecules, are: phytoplankton, non-pigmented particles (NPP, including inorganic and organic components), and chromophoric dissolved organic matter (CDOM).

* Corresponding author at: INIDEP, Mar del Plata, Argentina

E-mail addresses: vlutz@inidep.edu.ar (V. Lutz), rfrouin@ucsd.edu (R. Frouin), negri@inidep.edu.ar (R. Negri), risilva@inidep.edu.ar (R. Silva), pompeu@usp.br (M. Pompeu), natalia.rudorff@cptec.inpe.br (N. Rudorff), andersoncabral@yahoo.com.br (A. Cabral), adogliotti@iafe.uba.ar (A. Dogliotti), gumartin@minagri.gob.ar (G. Martinez).

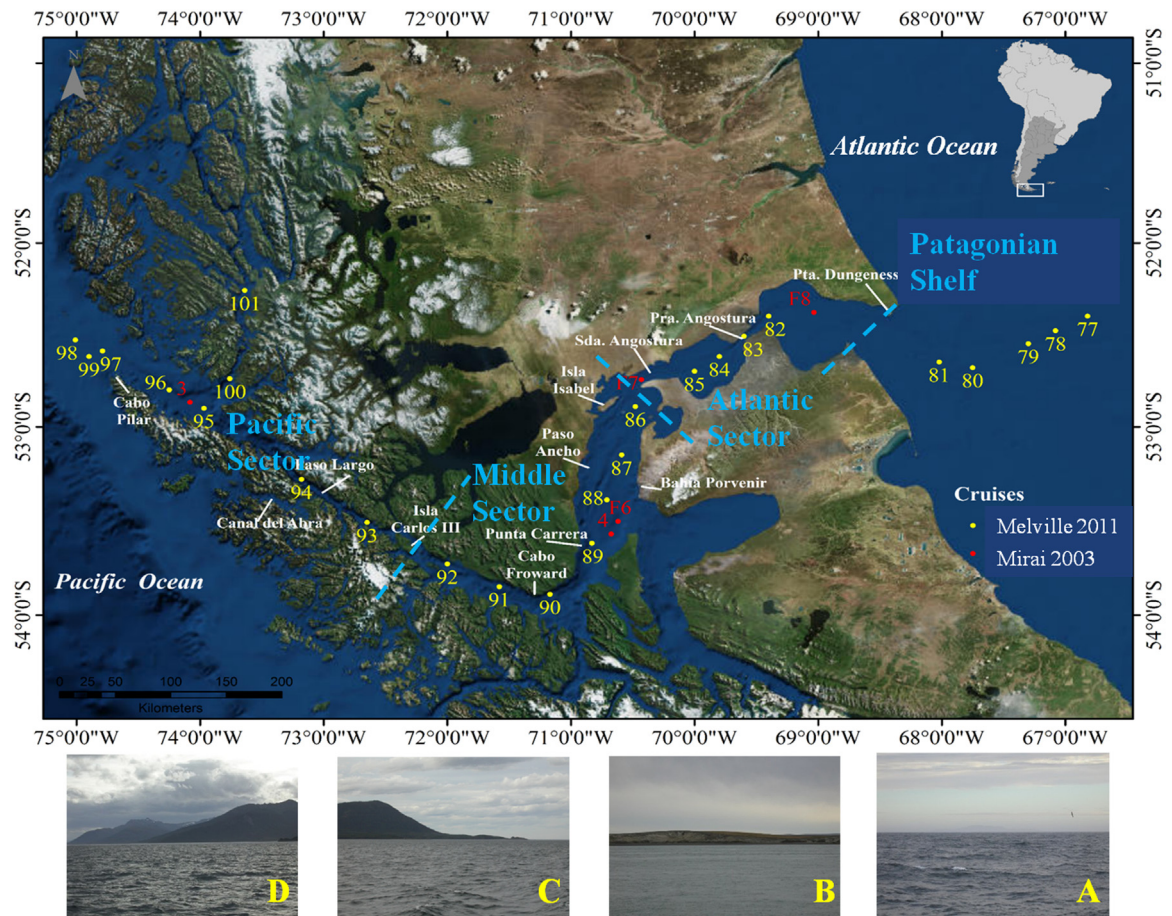


Fig. 1. Map of the Magallanes region, showing the position of the stations in both cruises (Mirai 2003 and Melville 2011). The cyan dashed-lines indicate the approximate limits of the sectors. The bathymetry and some geographical points are marked. Below are photos taken during the MV1102 cruise at the different sectors: (A) Patagonian Shelf, (B) Atlantic Sector, (C) Middle Sector, (D) Pacific Sector. (For interpretation of the references to color in this figure, the reader is referred to the web version of this article.)

The Straits of Magallanes is one of the important passages of the world ocean connecting two main basins, i.e., the Atlantic and the Pacific. Since the beginning of commercial transportation, it has provided a convenient way of crossing the southern oceans avoiding the risky Cape Horn. Artisanal fisheries as well as aquaculture enterprises are developed in its waters. The Straits is approximately 570 km long with a width ranging from 4 to 37 km, and it separates the southern tip of mainland South America from the island of Tierra del Fuego (Fig. 1). Plankton within the Straits is subjected to extremely dynamic changes, imposed by physical and geo-chemical conditions. The waters from the Straits have also a pronounced influence on the adjacent shelf. Numerical circulation models have indicated that the Magallanes plume spreads into the Atlantic forming what is known as the “Patagonian Current” flowing northeast in the middle of the Argentine shelf; its extension, being mainly regulated by the tides at the entrance of the Straits, usually reaches up to $\sim 42^{\circ}\text{S}$ (Palma and Matano, 2012).

Water optical properties, measured *in situ* and obtained by remote sensing, provide basic information on the environment which conditions phytoplankton physiology and hence the biological production. Although several hydrographic, geo-chemical and plankton studies have been conducted in the area of the Straits of Magallanes, bio-optical information is still scarce. This region is mostly cloudy year-around, hence remote sensing information on water-leaving radiance is hard to obtain, making *in situ* studies even more relevant.

The main objective of this work is to analyze the variability in the characteristics of the absorption by phytoplankton, non-pigmented particles, and CDOM observed along the Straits of

Magallanes in late summer 2011, and to discuss them according to environmental conditions and pigment and phytoplankton composition. As a comparison, a few results available from spring 2003 are also discussed. The main hypothesis is that persistent low light is a major factor conditioning phytoplankton distribution and physiology along the Straits.

2. The Straits of Magallanes: background

At the Atlantic entrance of the Straits, the landscape is dominated by the arid Patagonian terraces and the annual precipitation is ~ 300 mm. At the Pacific opening, the barrier to the winds provided by the Andes results in an average precipitation > 5000 mm per year, concomitant with a profuse austral forest; at this end, melting of glaciers in spring and summer also produce an important input of fresh water into the Straits (Panella et al., 1991). As a result light availability is substantially lower in the Pacific side than in the Atlantic side (Saggiomo et al., 1994). This contrast defines one of the most extreme climate divisions in the world (Aravena and Luckman, 2009). The coast on both borders is highly indented getting progressively more intricate towards the west, forming fjords, inlets and small basins including some small islands. The bathymetry is also highly variable ranging from ~ 30 m to ~ 1100 m of depth (Fig. 1). Within the Straits, the presence of elevations in the bathymetry constricts the circulation of Sub-Antarctic Water from the Pacific and the tidal mixing from the Atlantic, creating semi-enclosed environments (Aracena, et al., 2011). Although more complex spatial partitioning have been

proposed, three main sectors can be distinguished (Panella et al., 1991) according to the prevalent regimes (Fig. 1): (1) the 'Atlantic Sector' from the eastern entrance to the Segunda Angostura, dominated by strong tides (up to 8.5 m, with tidal currents up to 4.5 m s^{-1} ; Medeiros and Kjerfve, 1988) that homogenize the water column; (2) the 'Middle Sector' including Paso Ancho from the Segunda Angostura ($\sim 30 \text{ m}$ deep) to the sill close to Isla Carlos III ($\sim 64 \text{ m}$ deep), where physical forces are relatively smaller allowing a longer retention time of the water and the development of a seasonal thermocline in spring-summer; and (3) the 'Pacific Sector' from Isla Carlos III to the Pacific opening along the Paso Largo (up to 1100 m deep), where the westerly winds favor the entrance of Pacific waters from the Cape Horn Current (southern branch of the West Wind Drift current) into the Straits above the sill close to Cape Pilar ($\sim 60 \text{ m}$ deep). The water column here is mostly homogeneous, except for a thin superficial halocline induced by the input of fresh water from melting glaciers as well as frequent rains (8/10 days) (Panella et al., 1991; Aracena et al., 2011).

Salinity has been found to range from 28 to 32.5 PSU generally decreasing from the Atlantic to the Pacific (Panella et al., 1991). Regarding nutrients availability, spatial and temporal variations exist along the Straits (Saggiomo et al., 1994; Torres et al., 2011). Silicic acid, in particular, exhibits a higher variability due to terrestrial input and consumption by diatoms. The complex hydrography in the fjords (Valle-Levinson et al. 2006; Aracena et al., 2011), where salinity is the lowest, produces differences in stratification and nutrients availability.

Research conducted in late summer 1991 showed that the Atlantic and Pacific sectors had the lowest chlorophyll-*a* concentrations (Chla) ($< 1 \text{ mg m}^{-3}$), while the eastern part of Paso Largo (eastern of Pacific Sector) and the Middle Sector, subjected to the development of a pycnocline, had higher concentrations ($> 2 \text{ mg m}^{-3}$) (Saggiomo et al., 1994). The highest biomass was observed at the eastern side of the Middle Sector (from Cape Froward to Isla Isabel), and the predominant groups were Cryptophytes, small dinoflagellates, Prasinophytes, and small diatoms (Zingone et al., 2011).

In autumn 1995 surface Chla ranged from $< 0.2 \text{ mg m}^{-3}$ (slightly northeast from Cape Froward) to 0.9 mg m^{-3} (Bahía Porvenir, eastern shore of Paso Ancho) (Saggiomo et al., 2011). At that time, most of the phytoplankton was small in size, 46% and 27% of the total Chla were contributed by cells $< 2 \mu\text{m}$ and $< 10 \mu\text{m}$ respectively, where cyanobacteria dominated the picofraction and Prasinophytes, Prymnesiophytes, Cryptophytes and small diatoms were abundant in the nano-fraction (Vanucci and Mangoni, 1999). Intensive toxic blooms of *Gymnodinium* have also been recorded during autumn in different areas of the Straits from Canal Abra (in the Paso Largo, Pacific Sector) and Punta Carrera (in Paso Ancho, Middle Sector), causing problems in local fisheries (Uribe and Ruiz, 2001).

In spring 1989 nanoflagellates predominated in the Atlantic Sector, diatoms in the Middle one, and dinoflagellates in the Pacific Sector (Cabrini and Fonda Umani, 1991). Antezana and Hamamé (1999) found also that the spring bloom in 1994 was composed mainly by chain-forming diatoms at a site on Paso Ancho (Middle Sector) and that wind conditions, regulating the mixing in the upper water column, had a strong impact in the development of phytoplankton biomass (varying from 3 to 6 mg m^{-3} of Chla at the sub-surface). Iriarte et al. (2001) followed the composition of the phytoplankton community from spring to autumn (1997/1998) at several fixed stations in Paso Ancho, and found again that chain-forming diatoms dominated in spring (maximum Chla $\sim 2.5 \text{ mg m}^{-3}$) while phytoflagellates (especially Euglenophytes) dominated in summer (maximum Chla $< 0.5 \text{ mg m}^{-3}$).

3. Methods

3.1. Sampling and measurement of physical variables

R/V Melville sailed from Cape Town (South Africa) to Valparaíso (Chile) from February 20 to March 14, 2011 (MV0211 cruise). The region here analyzed was crossed from March 7–9, and 26 sites were sampled at sub-surface (yellow symbols in Fig. 1). Temperature and salinity were determined continuously by a thermo-salinographer attached to the flow-through circulation system ($\sim 4 \text{ m}$). At chosen sites seawater samples were drawn from the flow-through system, or from the 1 m bottle of Rosette casts, for on board CDOM absorption measurements. Aliquots of known volumes were filtered at low pressure ($< 5 \text{ psi}$) and dim light onto 25 mm diameter glass fiber GF/F Whatman filters, stored immediately in liquid nitrogen and later in an ultra-freezer ($-84 \text{ }^\circ\text{C}$) until analysis for chlorophyll-*a* concentration (at 26 sites), phytoplankton pigments composition (at 21 sites) and absorption coefficients (at 21 sites). Additionally at 6 selected sites 150 ml of seawater were fixed with neutralized paraformaldehyde (0.4% final concentration) for the analysis of phytoplankton composition under microscope, and other aliquots of 2 ml were fixed with 2% paraformaldehyde solution and kept in cryovials in liquid nitrogen until flow cytometric analysis.

The R/V Mirai 2003–2004 cruise around the world (BEAGLE expedition organized by the Japan Marine Science and Technology Center) also crossed the Straits of Magallanes on the 24 and 25 of October 2003. Temperature and salinity was determined continuously from the flow-through system ($\sim 4 \text{ m}$). Five sites were sampled (red symbols in Fig. 1) from the surface with a bucket or from the flow-through system for CDOM absorption measurements, and as for the MV2011 cruise aliquots of known volumes were filtered for phytoplankton pigments (stored in liquid nitrogen until analysis) and absorption (measured immediately on board).

3.2. Photosynthetically active radiation

Satellite-derived photosynthetically active radiation (PAR), defined as the quantum energy flux from the Sun in the spectral range 400–700 nm reaching the ocean surface, was obtained from NASA's Ocean Biology Processing Group using algorithms described in Frouin et al. (2003) and Frouin et al. (2012). The PAR data, in the form of daily (24-hour averaged) values at 4 km resolution from the MODerate resolution Imaging Spectroradiometer (MODIS) onboard Aqua and Terra, were temporally averaged to yield the PAR conditions in the Straits of Magallanes and surrounding oceans during March 6–13, 2011, the period during which MV1102 water samples were collected. Monthly values during the course of 2011 were also generated at 4 locations to provide information on seasonal PAR variations in the Pacific, Atlantic, and Middle Sectors of the Straits, and the Patagonian Shelf. PAR root-mean-squared accuracy is about $2 \text{ mol quanta m}^{-2} \text{ d}^{-1}$ on monthly estimates (Frouin et al., 2012).

3.3. Phytoplankton composition

3.3.1. Microscopy

The identification and quantification of the phytoplankton cells ($\sim 3\text{--}100 \mu\text{m}$), were made using an inverted microscope (Olympus IX70) by the sedimentation method (100 ml) (Utermöhl, 1958) at the "Instituto Nacional de Investigación y Desarrollo Pesquero (INIDEP)". The cells were grouped according to their classes i.e., diatoms (Bacillariophyceae), dinoflagellates (Dinophyceae), calcareous and non-calcareous haptophytes (Prymnesiophyceae), prasinophytes (Prasinophyceae), and separated into size classes of

pico ($< 2 \mu\text{m}$), nano ($2\text{--}20 \mu\text{m}$) and micro ($> 20 \mu\text{m}$) (Sieburth et al., 1978).

3.3.2. Flow cytometry

Identification and quantification of heterotrophic bacteria (HB), picoautotrophic eukaryotes (EUK), and Cyanobacteria (*Synechococcus* - SYN and *Prochlorococcus* - PROC) was performed by flow cytometry at the “Universidade Federal do Rio de Janeiro (UFRJ)” according to the method of Marie et al. (2005). The concentrations of each group were calculated in units of cells.ml^{-1} .

3.3.3. Estimation of phytoplankton carbon biomass

First, cellular biovolume was estimated using geometric shapes from digital images (Hillebrand et al., 1999). Then the carbon concentration from cell volumes of micro- and nano-plankton fractions was calculated using the equations proposed by Menden-Deuer and Lessard (2000). For picophytoplankton biomass was estimated using published conversion factors from cell volume to carbon: $0.22 \text{ pg C } \mu\text{m}^{-3}$ (Booth, 1995) for eukaryotic cells $< 5 \mu\text{m}$ and $0.21 \text{ pg C cell for } \textit{Synechococcus}$ cells of $0.8\text{--}1.5 \mu\text{m}$ (Waterbury et al., 1986).

3.4. Phytoplankton pigments

3.4.1. Spectrofluorometric determination of chlorophyll-*a* concentration

Chlorophyll-*a* concentration (Chl_a) for the R/V Melville cruise was determined by spectrofluorometry at INIDEP laboratory following the method of Holm-Hansen et al. (1965) modified by Lutz et al. (2010).

3.4.2. High performance liquid chromatography (HPLC) determination of pigment concentrations

The pigment composition of MV11012 samples was identified and quantified by HPLC. C. Thomas at NASA Goddard (Horn Point Laboratory, USA) performed the analysis, following Van Heukelem and Thomas (2001). Pigment samples from the Mirai 2003 cruise were analyzed by HPLC by L. Clementson at CSIRO laboratory (Australia), following Wright et al. (1991); data retrieved from SeaBASS (<http://seabass.gsfc.nasa.gov/seabasscgi/search.cgi>).

3.5. Absorption coefficients

3.5.1. Determination of particulate absorption coefficients

Replicate samples for the determination of particulate absorption coefficients for the R/V Melville cruise were analyzed at the “Instituto Oceanográfico da Universidade de São Paulo (IO-USP)” and INIDEP, following the quantitative filter technique (Mitchell 1990; Mitchell et al., 2002). Filters were placed on a quartz plate in a double beam Shimadzu UV-2450 spectrophotometer and optical density (OD) was recorded from 300 to 800 nm for the total particulate material. The filters were then extracted with methanol and read again to get the OD of non-pigmented particles (Kishino et al., 1985). These values of OD were corrected for a null absorption (subtracting from the whole spectrum the average OD from 790 to 800 nm) and for the path length amplification factor. Then, the absorption coefficients for the total particulate, $a_p(\lambda)$, and non-pigmented particles, $a_{NPP}(\lambda)$, were estimated converting \log_{10} into \log_n , and taking into account the effective filtration area and the volume of seawater filtered. Finally, the absorption coefficient of phytoplankton, $a_{ph}(\lambda)$, was obtained by subtracting the NPP absorption from the total particulate absorption.

The procedure followed for samples from the R/V Mirai cruise was similar than the one used for those of the R/V Melville cruise, except that samples were read immediately on board using a Cary-50 UV-vis-NIR (an average of 10 readings were taking for each

spectrum). One sample (collected at site F8) of total particulate absorption was processed using the mathematical approach of Hoepffner and Sathyendranath (1993) to estimate the phytoplankton and NPP absorption since, due to the high amount of sediments present, it was difficult to retrieve an appropriate phytoplankton spectrum using Kishino's method.

3.5.2. Determination of Chromophoric dissolved organic matter (CDOM) absorption coefficient

CDOM absorption determinations for both R/V Melville and R/V Mirai cruises were performed in the same way immediately on board following the method of Mitchell et al. (2002). Duplicate samples of seawater were filtered through acid-clean Nuclepore $0.2 \mu\text{m}$ filters, and read in 10 cm quartz cuvettes from 250 to 750 nm using a Cary-50 UV-vis-NIR spectrophotometer, using ultrapure MilliQ water as a reference. The CDOM absorption coefficients were calculated converting \log_{10} into \log_n , and taking into account the path length of the cuvette. More details of the process can be found in Ruddorf et al. (2014).

3.6. Euphotic depth

The depth of the euphotic layer (Z_{eu}), defined here as the depth where irradiance equals 1% of the surface irradiance, was estimated as $Z_{eu} = 4.6/K_d(\text{PAR})$ according to Kirk (1994). Where $K_d(\text{PAR})$ is the downwelling attenuation coefficient of underwater light, here parameterized according to Sathyendranath and Platt (1988). The inputs for this model were: the absorption and scattering spectra of pure seawater (Pope and Fry, 1997), the Chl_a values, $a_{NPP}(\lambda)$, $a_{ph}(\lambda)$, and $a_y(\lambda)$ here measured.

4. Results and discussion

4.1. Straits of Magallanes in late summer 2011

4.1.1. Variations in light

Although irradiance was recorded on board, instant measurements are subjected to large variability (due to wind inducing cloud covering), and the crossing of the Straits occurred partly during the night. Hence, to have a broad picture of light conditions at the time of the cruise a March 6-13, 2011 MODIS composite image of PAR was generated and is displayed in Fig. 2. Daily PAR values decreased from the Patagonian Shelf towards the Pacific Sector, as it is typical for the area. The Andes offer a barrier to the Southern Westerly Winds resulting in an annual precipitation $> 5000 \text{ mm}$ per year, making this area permanently cloud covered and drizzling. The eastern part, on the other hand, is drier and has relatively more clear skies (Aracena et al., 2011). Monthly variations in MODIS PAR throughout the year 2011 were followed for four selected points, one in each of the studied sectors (Fig. 3). The seasonal cycle of increasing irradiance towards summer is evident, while the pattern of decreasing values from the Patagonian Shelf towards the Pacific Sector is maintained for each month. Due to the limitation in the NASA processing to solar zenith angles less than 75° , PAR values are missing at the four locations during June and July and at the Pacific location also during May.

4.1.2. Distribution of salinity and chlorophyll-*a* concentration

Sea surface temperature (SST) had a low variation, ranging from 8.88°C (station 91, west of the Middle Sector) to 11.20°C (station 82, Atlantic Sector), and did not exhibit significant correlations with any of the other variables studied. This is within previous records of sea surface temperature, which showed a range from 4°C in September to 12°C in February (Iriarte et al., 2001). In this area, with variable influence of fresh-water input

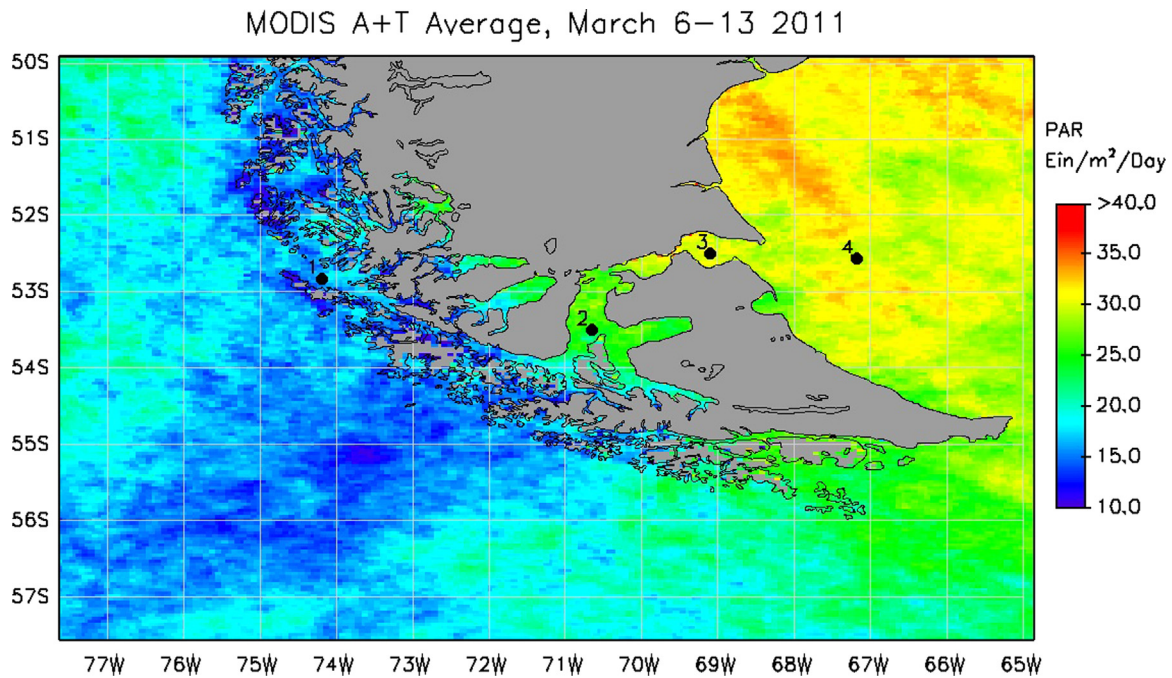


Fig. 2. Average daily incident irradiance (PAR) values distribution obtained using both MODIS Aqua and Terra for March 6–13 2011 (L3, 8-day composite, 4-km resolution). Dots show the location for which annual time series were extracted (see Fig. 3).

from glacier melting and precipitations, density was driven by salinity ($r_s=0.99$, Table 1). The trend showed high sea surface salinity (SSS) close to the Pacific (33.096, station 99) and Atlantic entrances and low SSS in the fjords area of the Pacific Sector (24.332, station 101) (Fig. 4), in agreement with previous reports

(Panella et al., 1991).

Chla was high in the Patagonian Shelf (up to 4.77 mg m^{-3}), abruptly decreased close to the Atlantic entrance of the Straits, started to increase in the Atlantic Sector, then decreased again on the east of the Middle Sector followed by a peak of 4.19 mg m^{-3} ,

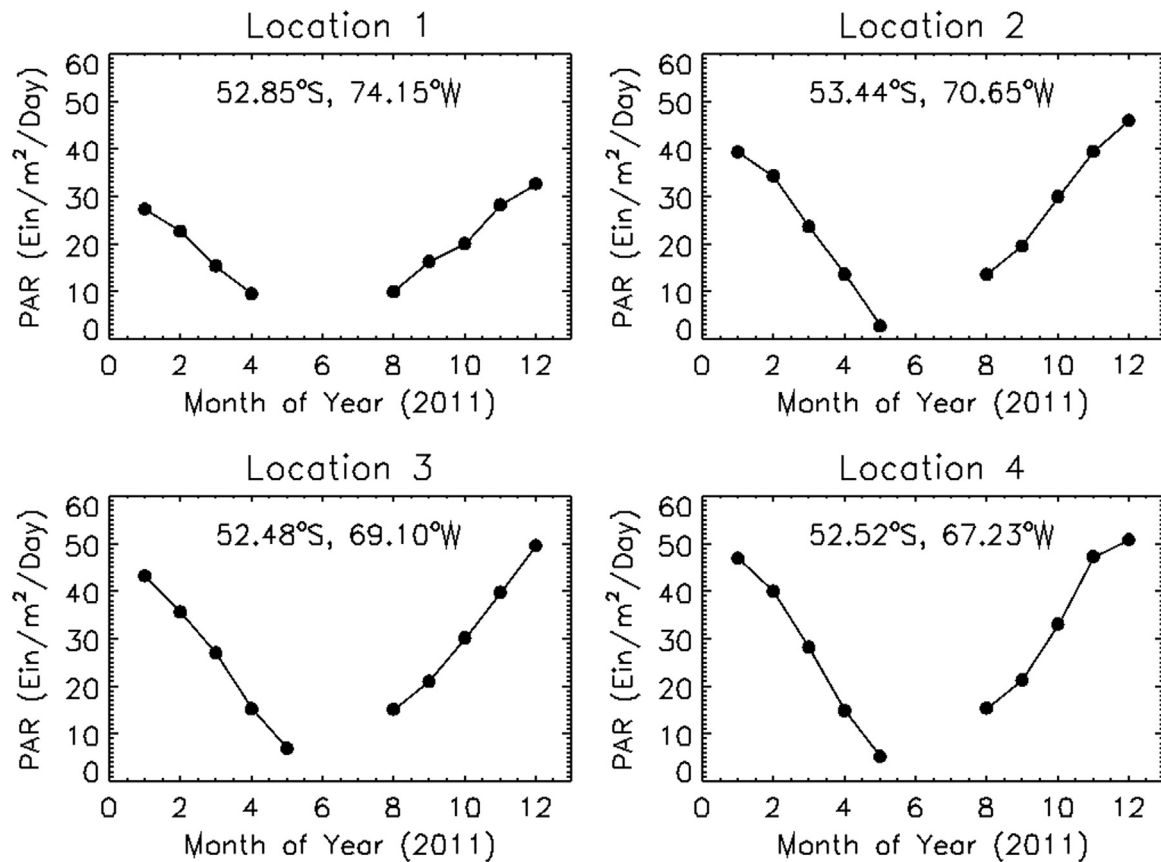


Fig. 3. Monthly average daily values of irradiance (PAR) throughout 2011, at 4 locations in the Straits of Magallanes (see positions in Fig. 2).

Table 1

Correlations among variables estimated from samples collected at the Straits of Magallanes in late summer 2011. Spearman correlation coefficients, probability values and number of samples are reported in each case.

	Sal	Fuco/Chla	Hex/Chla	Zea/Chla	[L+N+V]/Chla	$a_{ph}(440)$	$a_{NPP}(440)$	$a^*_{ph}(440)$
σ_T								
<i>r</i>	0.99							
<i>P</i>	0.000							
<i>n</i>	26							
Chla								
<i>r</i>	0.51							
<i>P</i>	0.008							
<i>n</i>	26							
Fuco/Chla								
<i>r</i>			−0.58					
<i>P</i>			0.006					
<i>n</i>			21					
Chlb/Chla								
<i>r</i>		−0.50		0.84	0.87			0.72
<i>P</i>		0.022		0.000	0.000			0.000
<i>n</i>		21		21	21			21
Zea/Chla								
<i>r</i>					0.83			0.60
<i>P</i>					0.000			0.000
<i>n</i>					21			21
[L+N+V]/Chla								
<i>r</i>								0.74
<i>P</i>								0.000
<i>n</i>								21
PPC/PSC								
<i>r</i>				0.84	0.81			0.67
<i>P</i>				0.000	0.000			0.000
<i>n</i>				21	21			21
$a_{ph}(440)$								
<i>r</i>	0.52							
<i>P</i>	0.010							
<i>n</i>	24							
$a_{NPP}(440)$								
<i>r</i>	0.45					0.52		
<i>P</i>	0.027					0.009		
<i>n</i>	24					24		
$a^*_{ph}(440)$								
<i>r</i>	−0.98						−0.50	
<i>P</i>	0.000						0.044	
<i>n</i>	16						16	

and from there values decreased towards and along the Pacific Sector with slightly higher concentrations at the entrance (Fig. 4), coincident to what was found for late summer 1991 (Saggiomo et al., 1994). There was a weak positive correlation between Chla and SSS, indicating that phytoplankton was more abundant in more saline seawaters than in the less saline waters of the fjords (Table 1). This is probably not due exclusively to the direct effect of salinity, but rather to a combination of co-varying factors, such as availability of nutrients and light. In the fjord area of the Pacific Sector, a characteristic shallow stratification is produced by the input of fresh colder water from the glaciers rich in silicic acid (and inorganic glacial-silt from erosion) and by a deeper layer of oceanic Sub-Antarctic water rich in nitrates (Valle-Levinson et al.

2006; Aracena et al., 2011).

4.1.3. Main phytoplankton groups

Total carbon concentrations estimated by microscopic and flow cytometric measurements ranged between 5.06 mg m^{-3} (st. 92, Middle Sector) and 49.06 mg m^{-3} (st. 76, Patagonian Shelf) (Fig. 5A). The carbon biomass was composed in its majority by the pico-fraction ($< 2 \mu\text{m}$) of phytoplankton and secondly by the nano-fraction ($2\text{--}20 \mu\text{m}$), with exception of the Atlantic Sector where the micro-fraction ($> 20 \mu\text{m}$) dominated at station 85 and was the second contributor at station 82 (Fig. 5B). Although total C showed a significant regression with Chla for the selected stations ($r^2=0.88$, power of the test 0.85, $n=6$), the C:Chla ratio showed a

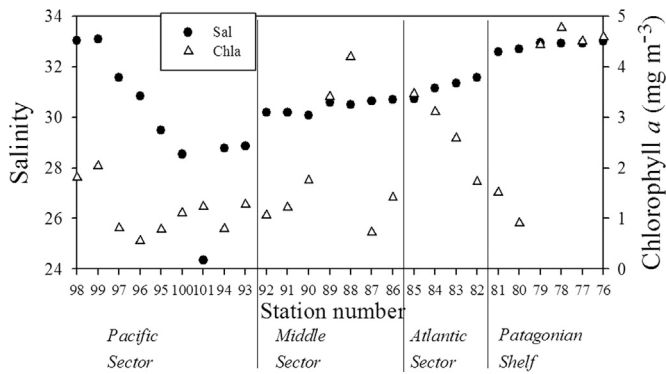


Fig. 4. Surface values of salinity and chlorophyll-*a* concentrations at the stations sampled during the MV1102 cruise.

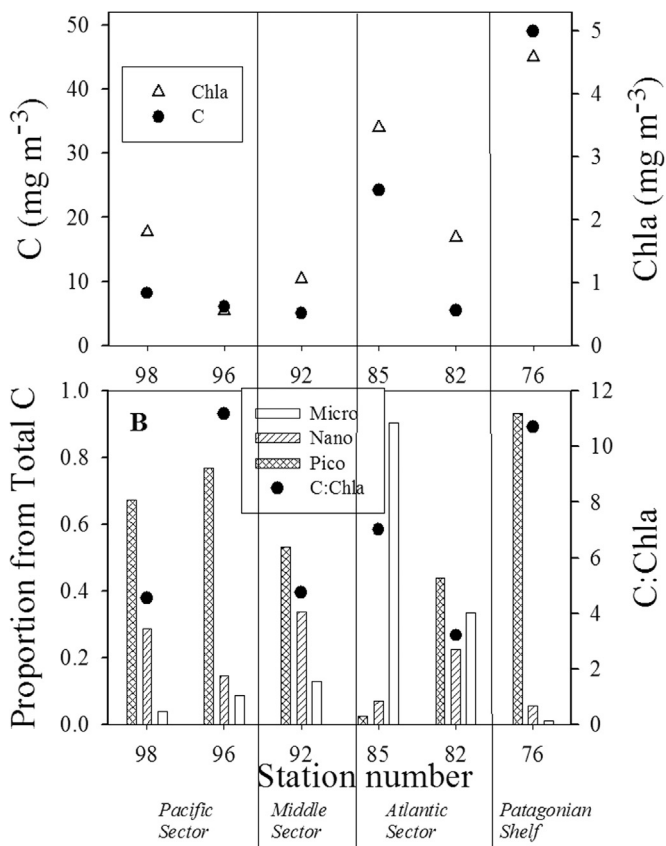


Fig. 5. A. Carbon and chlorophyll-*a* concentrations; B. Proportion of carbon in each of the size fractions with respect to the total carbon, and ratio total carbon to chlorophyll-*a*. All of them are surface values at selected stations during the MV1102 cruise.

large variability between 3.2 (st. 82) and 11.2 (st. 96) (Fig. 5B). The C:Chla ratio had a positive regression with the proportion of the pico-fraction when values from station 85 were left aside ($r^2=0.77$, power of the test 0.48, $n=5$), though due to the few data considered the power of the test fell below the desired value of 0.8 and hence the association should be interpreted with caution. This trend is in accordance to what has been observed regarding an increase in the ratio with decrease in cell-size (Geider, 1987; Sathyendranath et al., 2009). On the other hand, the values of the C:Chla ratio found here are low in comparison to those reported in the literature (mostly between 20 and 200; reviewed in Geider, 1987; Sathyendranath et al., 2009). These ratios were calculated using Chla determined spectrofluorometrically, the use of the slightly lower Chla values determined by HPLC did not cause any

substantial change (the higher C:Chla would raise from 11.2 to 15.6). The C:Chla ratio depends on the phytoplankton groups present (Llewellyn and Gibb, 2000; Chang et al., 2003) and even more on the physiological state of the cells (Geider, 1987). It has been reported that C:Chla decreases with a decreasing irradiance (due to photoacclimation increasing the intracellular concentration of pigments) and increases with a decreasing temperature (Geider, 1987; Geider et al., 1997). Although the low temperature in these waters would suggest a high C:Chla value, this effect may be overruled by the photoacclimation to a permanent low light environment, which seems to be the major factor affecting phytoplankton in this region. Most studies on C:Chla ratios (where C accounts for phytoplankton alone) have been performed with cultures from species collected usually from temperate or even sub-tropical environments. A low value of C:Chla (~ 4) for phytoplankton in the Paso Ancho area in summer could be derived from the work of Iriarte et al. (2001; their Table 1: mean Chla = 0.45 mg m^{-3} , sum of phytoplankton C = 1.80 mg m^{-3}). Previous evidence of a low C:Chla ratio (~ 12) was reported for an ice phytoplankton bloom in Antarctica (Bunt and Lee, 1972), while variations in C:Chla between 4.8 and 187.7 were found for the ultraphytoplankton ($< 5 \mu\text{m}$) at the EPEA station in the north coast of Argentina (Silva et al., 2009).

There was a rich diversity in phytoplankton groups among the different size-fractions (Fig. 6). Within the micro-fraction phytoplankton C was mainly composed by diatoms, except at station 76 (Patagonian Shelf) where dinoflagellates dominated and station 96 (Pacific Sector) where Euglenophytes were equally important (Fig. 6A). The nano-fraction C biomass was the most diverse in phytoplankton groups: diatoms had the highest contribution at stations 76 (Patagonian Shelf), 85 (Atlantic Sector) and 98 (Pacific Sector); calcareous haptophytes (mainly the coccolithophore *Emiliania huxleyi*) dominated at station 82 (Atlantic Sector) and 96 (Pacific Sector) and were second in contribution at station 92 (Middle Sector); dinoflagellates dominated this fraction at station 92 (Middle Sector) and were second at station 76 (Patagonian Shelf); and Prasinophytes and non-calcareous haptophytes had minor contributions at the different stations (Fig. 6B). Finally, the prevalent size-class at this time of the year, the pico-fraction (Fig. 6C) was composed in first place by cyanobacteria (*Synechococcus* sp.), except at station 85 (Atlantic Sector) where picophytoeukaryotes were equally important; this last group was the second component of the fraction and encompasses a variety of taxa (here dominated in most cases by green coccal cells). These results are comparable to those reported by Zingone et al. (2011), who found in late summer 1991 that micro-phytoplankton and large nano-phytoplankton ($10\text{--}20 \mu\text{m}$) were only relatively important (in terms of carbon biomass) in the two extremes, being represented mainly by diatoms in the Atlantic sector and by dinoflagellates in the Pacific Sector, while small nano-phytoplankton ($< 10 \mu\text{m}$) and pico-phytoplankton ($< 3 \mu\text{m}$) were predominant along the Straits.

Abundance of *Synechococcus* has been previously reported for the area (Vanucci and Mangoni, 1999), as well as for other high latitude environments (Vezina and Vincent 1996; Putland, 2000; Wilmotte et al., 2002; Huang et al., 2012; Pittera et al., 2014). Genetic tools are being used nowadays to describe different types (clades, ecotypes, strains) of *Synechococcus*, which have different physiological capacities to acclimate to different environmental conditions. This genetic diversity explains the widespread global distribution of *Synechococcus*, and would render this genus well suited to adapt to changes occurring in the ocean (Zwirgmaier et al., 2008; Mackey et al., 2013; Flombaum et al., 2013; Jodłowska and Sliwiska, 2014; Pittera et al., 2014; Perez-Cenci et al., 2014).

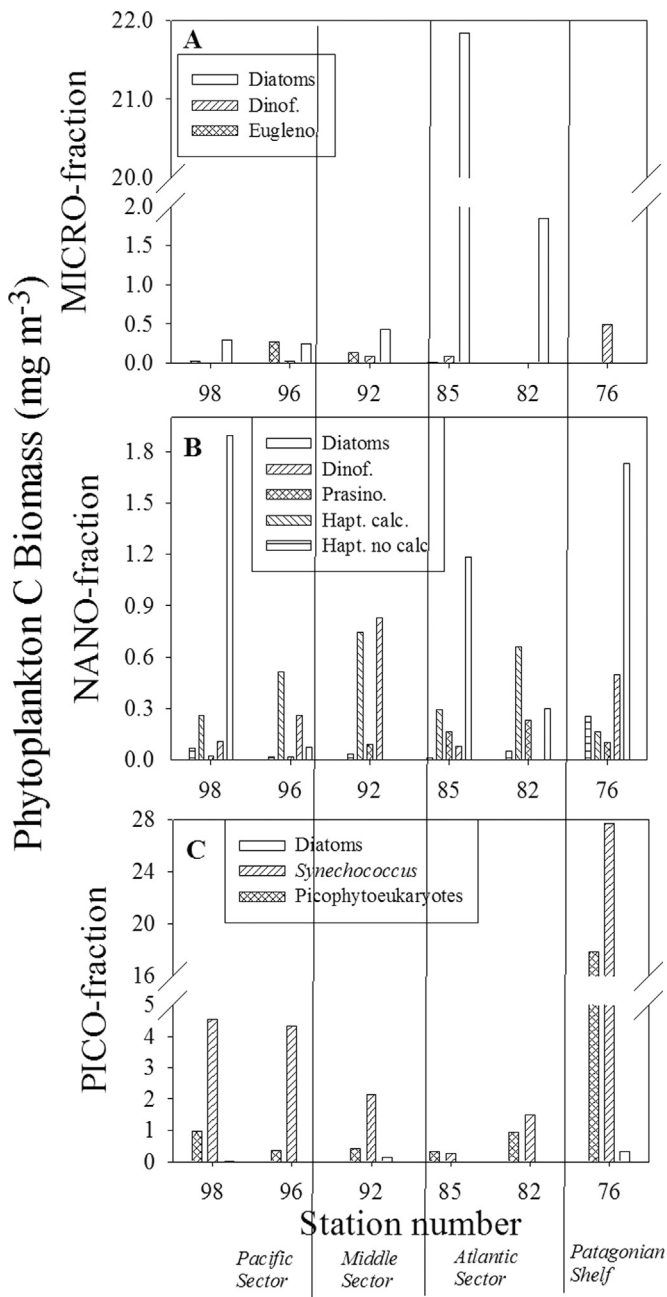


Fig. 6. Surface carbon concentrations, at selected stations during the MV1102 cruise, for the main taxonomic components within each size fraction: A. microphytoplankton; B. nanophytoplankton; C. picophytoplankton.

4.1.4. Main phytoplankton pigments

The $\text{Chlc}_{1+2}:\text{Chla}$ ratio (indicative of red algae; i.e., diatoms, dinoflagellates, haptophytes, rhodophytes, cryptophytes, chrysophytes, etc.) was the highest among the accessory chlorophylls at stations in the Atlantic Sector, eastern stations in the Middle Sector and the two stations at the Pacific entrance. The ratio $\text{Chlb}:\text{Chla}$ (indicative of green algae; i.e., chlorophytes, euglenophytes, prasinophytes, etc.) was higher than the $\text{Chlc}_{1+2}:\text{Chla}$ at the rest of the stations, except at stations 76 and 77 (Patagonian shelf) where the two ratios were similar (Fig. 7A). The $\text{Chlc}_3:\text{Chla}$ ratio (indicative mainly of Haptophytes) exhibited values much lower than those for the other chlorophylls, only modestly higher on the Patagonian Shelf and at the Pacific entrance (Fig. 7A).

Fucoxanthin (Fuco), a main but not exclusive pigment in diatoms, was the major carotenoid as shown by high though variable

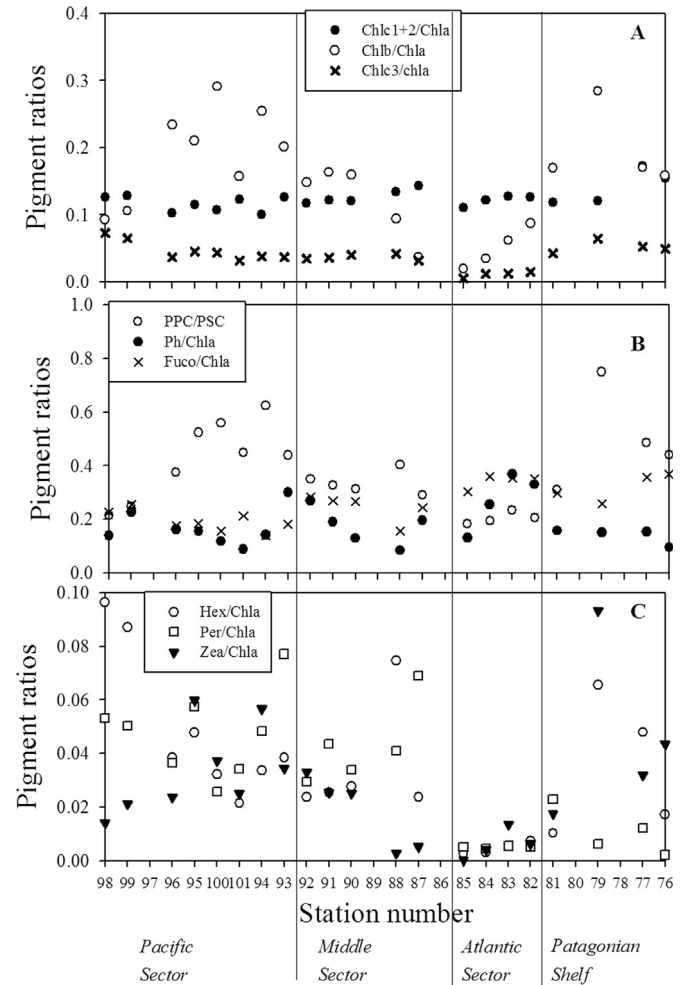


Fig. 7. Surface values of main pigments to chlorophyll-a ratios, at selected stations at the MV1102 cruise. A. Chlorophyll-*c*₁₊₂/chlorophyll-*a* ($\text{Chlc}_{1+2}:\text{Chla}$), chlorophyll-*b*/chlorophyll-*a* ($\text{Chlb}:\text{Chla}$), chlorophyll-*c*₃ ($\text{Chlc}_3:\text{Chla}$); B. [Sum of photoprotective carotenoids]/[sum of photosynthetic carotenoids] (PPC/PSC), [phaeophytin-*a* + phaeophorbide-*a*]/chlorophyll-*a* (Ph/Chla), fucoxanthin/chlorophyll-*a* (Fuco/Chla); C. 19'hexanoyloxyfucoxanthin/chlorophyll-*a* (Hex/Chla), peridinin/chlorophyll-*a* (Per/Chla), zeaxanthin/chlorophyll-*a* (Zea/Chla).

Fuco:Chla ratios at all stations (Fig. 7B). The other carotenoids had lower and variable ratios to Chla. Zeaxanthin (Zea), present in prokaryotes and green algae, had the highest Zea:Chla ratio at station 79 (Patagonian Shelf); 19'hexanoyloxyfucoxanthin (Hex), present mainly in Haptophytes, had the highest Hex:Chla ratios at the Pacific entrance and at station 88 (Middle Sector); while peridinin (Per), present in dinoflagellates, was a minor pigment, with the highest Per:Chla ratios at station 93 (east of Pacific Sector) and at station 87 (Middle Sector) (Fig. 7C).

At station 88 (Middle Sector) Chla was high (4.19 mg m⁻³), and although unfortunately no sample was taken for microscopy/flow-cytometry analysis, the pigment composition indicated a mixed phytoplankton composition. Here the pigment analysis showed relatively lower Fuco:Chla and higher Hex:Chla and $\text{Chlc}_3:\text{Chla}$ ratios (than at the rest of the stations), suggesting the presence of Haptophytes, the relatively high Allo:Chla (not shown) indicated the presence of Cryptophytes, and a non-negligible Per:Chla ratio, indicated the presence of dinoflagellates (Fig. 7 B and C).

The Fuco:Chla ratio was negatively correlated to the Hex:Chla and $\text{Chlb}:\text{Chla}$ ratios, from which we can infer that diatoms were more abundant where haptophytes and green algae were not (Table 1). This can also be derived from the phytoplankton composition (Fig. 6). The ratio $\text{Chlb}:\text{Chla}$ was positively correlated

mainly to the Zea:Chla and [Lu+Neo+Vio]:Chla ratios, which were highly correlated to each other, since these pigments are common to green algae (here mostly represented by coccal green cells known to be an important component of the picophytoeukaryotes).

The proportion of photoprotective to photosynthetic carotenoids (PPC:PSC) provides an indication of both the photo-acclimation status and the variation in phytoplankton composition; i.e., a high PPC:PSC ratio would indicate acclimation to high irradiance, or the presence of species with permanent high PPC (i.e., prokaryotes and green coccal cells). Here the PPC:PSC ratio (Fig. 7B) had a strong correlation with both Zea:Chla and [Lu+Neo+Vio]:Chla ratios (Table 1), hence indicating the presence of prokaryotes and green algae rather than acclimation to high light, since surface irradiance was low during the time of sampling in the Straits (due to heavy cloud cover and drizzle).

Non-negligible amounts of degradation products from Chla, phaeopigments (Ph)=phaeophytin + phaeophorbide, were present, which can be related to several factors: grazing, presence of diatoms with high chlorophyllase activity, and re-suspension of sediments (containing dead or senescent phytoplankton). The Ph:Chla ratio was higher in the Atlantic Sector, where sediments – therefore the probability of finding senescent cells – were abundant, and at the limit between the Middle and Pacific Sectors (Fig. 7B). There was a weak correlation between the Ph:Chla ratio and the absorption coefficient of non-pigmented particles, $a_{NPP}(440)$, ($r_S \sim 0.38$, $P \sim 0.086$).

4.1.5. Comparison between taxonomy and pigment composition of the phytoplankton

Using the Uitz et al. (2006) pigment indices the proportion of the three main size-classes of phytoplankton (micro, nano and pico) was estimated at each station (values provided by the NASA laboratory). Independently, for the selected stations analyzed by microscopy and flow cytometry, the proportion of these size-classes was estimated according to the carbon biomass in each fraction (Fig. 8). Except at station 85, where diatoms from the micro fraction were dominant, the two kinds of size-class indices did not match. This is because the diatoms, abundant at some stations, were of small size (nano or pico fraction), while when using the pigment indices diatoms are assigned by default to the micro-fraction. Here the disparity was probably enhanced by photoacclimation of the diatoms to low light, increasing the intracellular concentration of the light-harvesting fucoxanthin, and of cyanobacteria decreasing the intracellular concentration of the photo-protective zeaxanthin. This result highlights the importance of counting with microscopic information when making inferences about cell sizes. (NASA does not longer report indices of size-fraction; C. Thomas pers. comm.).

Flow cytometry analysis indicated the presence of high

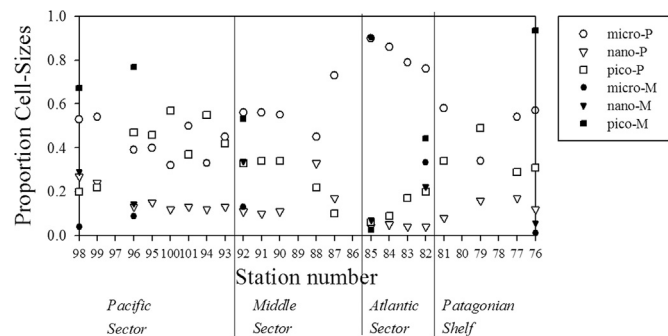


Fig. 8. Surface values of the proportion of each size class (micro-, nano- and pico-phytoplankton) to the total, as estimated by pigments (P) and microscopy & flow cytometry (M) analyses, at selected stations from the MV1102 cruise.

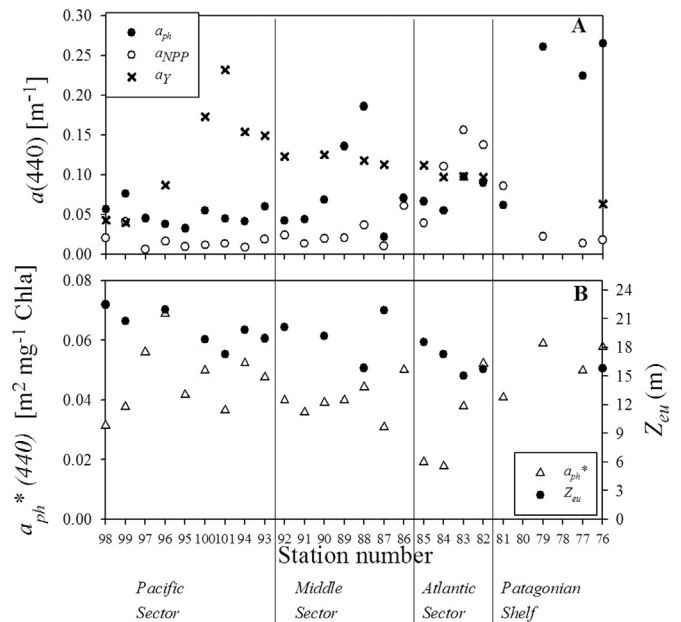


Fig. 9. A. Surface values of the absorption coefficients at 440 nm for phytoplankton, non-pigmented particles and CDOM; B. Specific absorption coefficient of phytoplankton at 440 nm and euphotic depth (Z_{eu}) at selected stations from the MV1102 cruise.

abundances of *Synechococcus* at several stations (Fig. 6C). Nevertheless, HPLC data showed relatively low concentrations of Zea. The Zea:Chla ratio for station 76, where *Synechococcus* was dominant, was 0.04 (even if we allocate only half of the Chla to *Synechococcus*, following the proportion of carbon in this group, the ratio would only increase to 0.08), while commonly the Zea:Chla ratio for *Synechococcus* ranges between ~ 0.2 – 2.0 according to acclimation (Kana et al., 1988, cultures; Lutz et al., 2003, field samples). This suggests that *Synechococcus* cells may have been adjusting their pigment proportions to particular conditions in this region due to the combination of cold waters and low light. It has been reported that some natural populations of cyanobacteria are able to convert zeaxanthin into its 7', 8'-dihydro derivative paraxanthin, which may have a role in membrane fluidity at low temperatures (in Scanlan et al., 2009).

4.1.6. Absorption by different components

There was a high variability in the absorption by different components along the region (Fig. 9A). In the Patagonian Shelf total absorption at 440 nm was dominated by the phytoplankton (at st. 76 $a_{ph}(440) = 0.265 \text{ m}^{-1}$ representing 76% of the total absorption [$a_{ph}(440) + a_{NPP}(440) + a_y(440)$]), while in the Atlantic Sector the major contributor was NPP (at st. 82; $a_{NPP}(440) = 0.138 \text{ m}^{-1}$ representing 42% of the total absorption), in the Middle Sector CDOM dominated at most stations except at the phytoplankton peak (around station 88), and in the Pacific Sector CDOM contributed up to 80% of the total absorption in the blue (at st. 101 $a_y(440) = 0.232 \text{ m}^{-1}$). The specific absorption coefficient of phytoplankton (representing a measure of efficiency of absorption per unit Chla) in the blue, $a_{ph}^*(440)$, was also highly variable along the Straits ranging from 0.018 to 0.069 $\text{m}^2 (\text{mg Chla})^{-1}$ (Fig. 9B). Here, the estimated euphotic depth, Z_{eu} , varied between 15 and 22 m (Fig. 9B), and according to the literature (Panella et al. 1991; Saggiomo et al. 1994) the depth of the mixed layer (Z_m) is usually deeper than 40 m at the Middle and Pacific Sectors while a completely homogeneous water column is observed at the Atlantic Sector. Therefore, since Z_{eu} seems to be shallower than the expected Z_m phytoplankton cells would be mixed down below the

illuminated layer. This is another factor contributing to the low light acclimation of phytoplankton in the Straits.

The absorption by phytoplankton and non-pigmented particles at 440 nm were positively correlated to salinity but weakly, while CDOM absorption was negatively correlated to salinity but strongly ($r_s = -0.98$, $P < 0.0001$) (Table 1). This is concordant to the fact that CDOM dominated the light absorption in the fresh-water influenced area of the fjords, while particles dominated in the more saline areas of the Straits (close to the two ocean entrances) and in the Patagonian Shelf.

The absorption by non-pigmented particles, $a_{NPP}(440)$ was positively correlated to $a_{ph}(440)$. In turn CDOM absorption, $a_y(440)$, was negatively correlated to $a_{NPP}(440)$, but not significantly correlated to $a_{ph}(440)$ (Table 1). This would be a further indication that CDOM originated mostly from land vegetation rather than plankton.

The $a_{ph}^*(440)$ was positively correlated to the ratios of Chlb:Chla, Zea:Chla, [Lu+Neo+Vio]:Chla and PPC:PSC (Table 1), indicating that small cells -known to have higher efficiency of light absorption per unit Chla- were mainly composed by prokaryotes and green algae in this region, as it was observed by microscopic/flow-cytometric and pigment analyses. The highest values of $a_{ph}^*(440)$ found here are in agreement to what is expected for pico-phytoplankton (Ciotti et al., 2002), though they were lower than those reported for a *Synechococcus* dominated population at EPEA during summer ($\sim 0.15 \text{ m}^2 \text{ mg Chla}^{-1}$) where cells were photoacclimated to high irradiance, probably with higher Zea concentration (Silva et al., 2009).

4.2. Straits of Magallanes in spring 2003

4.2.1. Salinity and pigments

In the five stations sampled during the R/V Mirai 2003 cruise salinity exhibited only a slight decrease in the Middle Sector (Fig. 10A). Chla was low in the Atlantic and Pacific Sectors (1.26 and 0.65 mg m^{-3} respectively) and $> 3.5 \text{ mg m}^{-3}$ on the Middle Sector (reaching 5.05 mg m^{-3} at st. 4) (Fig. 10A).

The $\text{Chlc}_{1+2}:\text{Chla}$ ratio was > 0.2 at all stations, except at st. F8 in the Atlantic Sector where it was lower (0.1), while the concentrations of the other accessory chlorophylls (b and c_3) were negligible, with only traces of Chlb at st. 3 in the Pacific Sector (Fig. 10B). Among the carotenoids the major one present was fucoxanthin, with a ratio $\text{Fuco}:\text{Chla}$ ranging between 0.25 and 0.34 (Fig. 10C) and traces of peridinin, prasinoxanthin, and alloxanthin at st. 3 in the Pacific Sector (not shown). The PPC:PSC ratio was relatively constant (ranging between 0.16 and 0.21), where the main PPC was diadinoxanthin (present mostly in diatoms). The degradation products of Chla could be detected in very low concentration relative to Chla only at two stations (maximum ratio $\text{Ph}:\text{Chla} = 0.07$ at st. F7) (Fig. 10C).

Unfortunately, there are no results available on phytoplankton composition for this section of the cruise. On the other hand, the pigment composition was less diverse than in the summer cruise, and suggests that diatoms dominated the phytoplankton at that time, as previously reported by Iriarte et al. (2001) and Decembrini et al. (2014).

4.2.2. Absorption by different components

During this spring period, phytoplankton contributed largely to the absorption at 440 nm, with a maximum $a_{ph}(440)$ value of 0.232 m^{-1} (st. F6, Middle Sector) (Fig. 11A). CDOM absorption dominated at two stations (in the Pacific and Middle Sector), but the $a_y(440)$ values were high everywhere (range: $0.126\text{--}0.165 \text{ m}^{-1}$), and NPP absorption was high only at st. F8 in the Atlantic Sector (Fig. 11A).

The specific absorption coefficient of phytoplankton at 440 nm

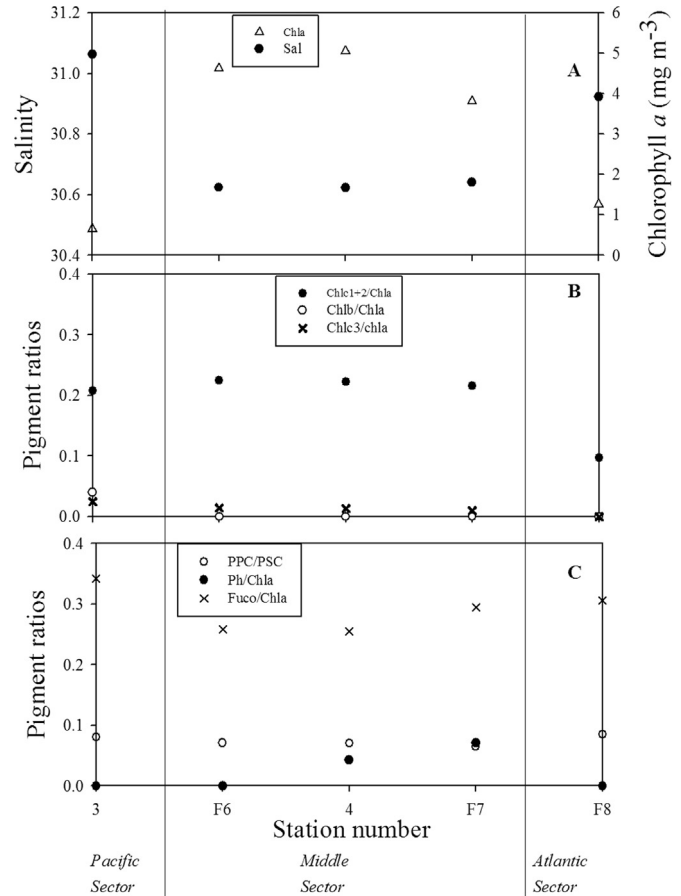


Fig. 10. Surface values of: A. Salinity and chlorophyll-*a* concentrations; B. chlorophyll-*c*₁₊₂/chlorophyll-*a*, chlorophyll-*b*/chlorophyll-*a*, chlorophyll-*c*₃; C. [Sum of photoprotective carotenoids]/[sum of photosynthetic carotenoids], [phaeophytin-*a*+phaeophorbide-*a*]/chlorophyll-*a*, fucoxanthin/chlorophyll-*a*, at the stations sampled during the Mirai 2003 cruise.

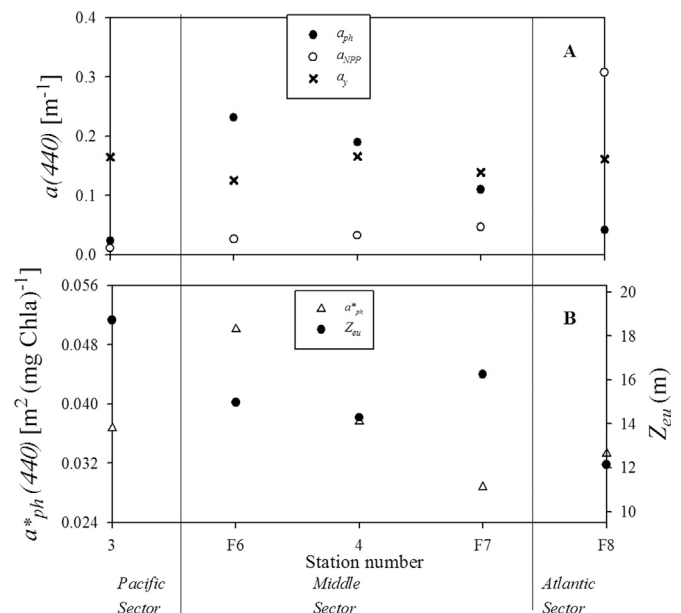


Fig. 11. Surface values of the absorption coefficients at 440 nm for phytoplankton, non-pigmented particles and CDOM and euphotic depth (Z_{eu}) at the stations sampled during the Mirai 2003 cruise.

ranged between 0.025 and 0.041 m² (mg Chl a)⁻¹ (Fig. 11B). These values are lower in average than those found in late summer 2011, suggesting again that during spring large diatoms were probably dominant in the phytoplankton. In spring the Z_{eu} was even shallower than at the end of summer, ranging between 12 and 19 m (Fig. 11B). This again points towards the need of phytoplankton to acclimate to low light, since the physical mixing most probably entrained the cells below the euphotic layer (according to the Z_m reported in Panella et al., 1991 and Saggiomo et al., 1994).

5. Concluding remarks

Water absorption along the Straits of Magallanes followed a progression tightly coupled to the longitudinal changes in geographical landscape. It was mainly dominated by phytoplankton in the rich Patagonian Shelf, by non-pigmented-particles in the Atlantic Sector with strong tides and heavy re-suspension of sediments, by phytoplankton and CDOM in the Middle Sector, and finally by CDOM towards the fjords influenced by glacier melting and forest runoff.

Our results confirm previous observations regarding phytoplankton composition, which was dominated by the pico fraction during late summer (2011) and by diatoms in early spring (2003). During summer, cyanobacteria contributed a large proportion of the phytoplankton carbon. The *Synechococcus* population exhibited a very distinct pigment composition, with high Chl a and low Zea concentrations, due to acclimation to the permanent low light and low temperature environment. This resulted also in very low values of the C:Chl a ratio (<15). Phytoplankton photoacclimation to low light must have been caused not only by the low irradiance, but also by the high absorption of underwater light by CDOM and NPP. This was evident in the fact that the euphotic depth, regulated by the attenuation coefficient of underwater light, was overall shallow. These findings support our hypothesis that light is a major forcing conditioning phytoplankton distribution and physiology in the Straits of Magallanes. The photoacclimation to low light also resulted in high Fuco:Chl a ratios for the relatively few diatoms present, producing a biased higher proportion of micro-phytoplankton when estimated by pigment indices. Presence of small nano and pico diatoms also biased the phyto-sized pigment model. Photoacclimation effects should be taken into account when applying biogeochemical models in this area.

It has been shown that different phytoplankton communities prosper in the varied environments along the Straits during late summer. Since there is a general flow of water towards the Atlantic, one would expect that variations occurring in phytoplankton communities, as well as CDOM and NPP, in the Straits would impact the Patagonian Shelf as the Magallanes plume carried them.

Finally, the study emphasizes how phytoplankton is acclimated in a fine equilibrium to its environment in this highly heterogeneous area. The Magallanes region, thought to be pristine due to its remoteness, is under strong anthropogenic influence, which affects the conditions for phytoplankton growth. This includes oil exploitation (a considerable number of oil rigs operate in the Straits), transport (one of the worst oil spills in history occurred in 1974 at the Primera Angostura), and salmon aquaculture (Aqua, 2014). Furthermore, climate change affecting glacier melting and the precipitation regime mainly in the west, and tidal forces as well as wind forces on the Middle and Atlantic Sectors, would produce changes in the mixing and hence in the phytoplankton dynamics of the Straits.

Acknowledgments

The crews of R/V Melville and R/V Mirai are gratefully acknowledged, as well as the help of our colleagues on board, especially Walter Grismayer. We are grateful to Shubha Sathyendranath for leading the bio-optical project of the R/V Mirai and to Masao Fukasawa for the organization of the whole expedition. The National Science Foundation and the Scripps Institution of Oceanography (SIO) provided ship time and logistics and technical support for the MV1102 cruise. We acknowledge funding received by INIDEP and CONICET. The National Aeronautics and Space Administration (NASA) supported R. Frouin under various grants. Dr Rodolfo Paranhos provided support and allowed the use of the cytometry Multi-User Unit (UCEA- IB/UFRJ). AC was funded by CAPES Post-doctoral fellowship (Edital Ciências do Mar 09/2009), and FAPERJ Post-doctoral fellowship (E-26/103.692/2012). We thank Crystal Thomas from NASA for performing HPLC pigment analysis for the MV1102 cruise, Gregg Mitchell and Brian Schieber from SIO for providing filtration equipments, as well as useful advice, and John McPherson from SIO and Eleonora Veron and Lucrecia Allegra from INIDEP for assistance. This is INIDEP contribution n° 1979.

References

- Antezana, T., Hamamé, M., 1999. Short-term changes in the plankton of a highly homogeneous basin of the Straits of Magellan (Paso Ancho) during spring 1994. *Sci. Mar.* 63, 59–67.
- Aqua, 2014. Vol 171 www.aqua.cl.
- Aracena, C., Lange, C.B., Iriarte, J.L., Rebolledo, L., Pantoja, S., 2011. Latitudinal patterns of export production recorded in surface sediments of the Chilean Patagonian fjords (41–55°S) as a response to water column productivity. *Cont. Shelf Res.* 31, 340–355.
- Aravena, J.C., Luckman, B.H., 2009. Spatio-temporal rainfall patterns in southern south America. *Int. J. Climatol.* 29, 2106–2120.
- Booth, B.C., 1995. Estimación de la biomasa del plancton autotrófico usando microscopía. In: *Manual De Métodos Ficológicos*. Alveal K, Ferrario ME, Oliveira EC, SAR E (eds). Universidad De Concepción, Chile, pp. 187–198.
- Bunt, J.S., Lee, C.C., 1972. Seasonal primary production in Antarctic sea ice at McMurdo sound in 1967. *J. Mar. Res.* 28, 304–320.
- Chang, J., Shiah, F.K., Gong, G.C., Chiang, K.P., 2003. Cross-shelf variation in carbon-to-chlorophyll *a* ratios in the east China Sea, summer 1998. *Deep-SEA Res. II* 50, 1237–1247.
- Ciotti, A.M., Lewis, M.R., Cullen, J.J., 2002. Assessment of the relationships between dominant cell size in natural phytoplankton communities and the spectral shape of the absorption coefficient. *Limnol. Oceanogr.* 47, 404–417.
- Cabrini, M., Fonda Umani, S., 1991. Phytoplankton populations in the strait of Magellan. *Boll. Oceanol. Teor. Appl.* 9, 137–144.
- Decembrini, F., Bergamasco, A., Mangoni, O., 2014. Seasonal characteristics of size-fractionated phytoplankton community and fate of photosynthesized carbon in a sub-Antarctic are (Straits of Magellan). *J. Mar. Syst.* 136, 31–41.
- Flombaum, P., Gallegos, J.L., Gordillo, R.A., Rincón, J., Zabala, L.L., Nianzhi, J., Karl, D. M., Li, W.K.W., Lomas, M.W., Veneziano, D., Vera, C.S., Vrugt, J.A., Martiny, A., 2013. Present and future global distributions of the marine cyanobacteria *Prochlorococcus* and *Synechococcus*. *PNAS* 110, 9824–9829.
- Frouin, R., Franz, B.A., Werdell, P.J., 2003. The SeaWiFS PAR product. In "Algorithm Updates for the Fourth SeaWiFS Data Reprocessing". Hooker SB, Firestone ER (eds), NASA/TM-2003-206892, 22:46–50.
- Frouin, R., McPherson, J., Ueyoshi, K., Franz, B., 2012. A time series of photosynthetically available radiation at the ocean surface from SeaWiFS and MODIS data. *Proc. SPIE* 8525, Remote Sens. Mar. Environ., 852519. <http://dx.doi.org/10.1117/12.981264>.
- Geider, R., 1987. Light and temperature dependence of the carbon to chlorophyll *a* ratio in Microalgae and cyanobacteria: implications for physiology and growth of phytoplankton. *New Phytol.* 106, 1–34.
- Geider, R., MacIntyre, L., Kana, T.M., 1997. Dynamic model of phytoplankton growth and acclimation: responses of the balanced growth rate and the chlorophyll *a*: carbon ratio to light, nutrient-limitation and temperature. *Mar. Ecol. Prog. Ser.* 148, 187–200.
- Hillebrand, H., Dürselen, C.D., Kirshtel, D., Pollinger, U., Zohary, T., 1999. Biovolume calculation for pelagic and benthic microalgae. *J. Phycol.* 35, 403–424.
- Hoepffner, N., Sathyendranath, S., 1993. Determination of the major groups of phytoplankton pigments from the absorption spectra of total particulate matter. *J. Geophys. Res.* 98, 22,789–22,803.
- Holm-Hansen, O., Lorenzen, C.J., Holmes, R.W., Strickland, J.D.J., 1965. Fluorometric determination of chlorophyll. *J. Cons.* 30, 3–15.

- Huang, S., Wilhelm, S.W., Harvey, H.R., Taylor, K., Jiao, H., Chen, F., 2012. Novel lineages of *Prochlorococcus* and *Synechococcus* in the global oceans. *ISME J.* 6, 285–297.
- Iriarte, J.L., Kusch, A., Osses, J., Ruiz, M., 2001. Phytoplankton biomass in the sub-antarctic area of the Straits of Magellan (53°S), Chile during spring-summer 1997/1998. *Polar Biol.* 24, 154–162.
- Jodłowska, S., Sliwiska, S., 2014. Effects of light intensity and temperature on the photosynthetic irradiance response Curves and chlorophyll fluorescence in the three Picocyanobacterial strains of *Synechococcus*. *Photosynthetica* 52, 223–232.
- Kana, T.M., Glibert, P.M., Goericke, R., Welschmeyer, N.A., 1988. Zeaxanthin and β-carotene in *Synechococcus* WH7803 respond differently to irradiance. *Limnol. Oceanogr.* 33, 1623–1627.
- Kirk, J.T.O., 1994. *Light and Photosynthesis in Aquatic Ecosystems*, Second edition. Cambridge University Press, Cambridge, p. 509.
- Kishino, M., Takahashi, M., Okami, N., Ichimura, S., 1985. Estimation of the spectral absorption coefficients of phytoplankton in the sea. *Bull. Mar. Sci.* 37, 634–642.
- Llewellyn, C.A., Gibb, S.W., 2000. Intra-class variability in the carbon, pigment and Biomineral content of Prymnesiophytes and diatoms. *Mar. Ecol. Prog. Ser.* 193, 33–44.
- Lutz, V.A., Sathyendranath, S., Head, E.J.H., Li, W.K.W., 2003. Variability in pigment composition and optical characteristics of phytoplankton in the Labrador Sea and the Central North Atlantic. *Mar. Ecol. Prog. Ser.* 260, 1–18.
- Lutz, V.A., Segura, V., Dogliotti, A.I., Gagliardini, D.A., Bianchi, A.A., Balestrini, C.F., 2010. Primary production in the Argentine Sea during Spring estimated by field and satellite models. *J. Plankton Res.* 32, 181–195.
- Mackey, K.R.M., Paytan, A., Caldeira, K., Grossman, A.R., Moran, D., McIlvin, M., Saito, M.A., 2013. Effect of temperature on photosynthesis and growth in marine *Synechococcus* spp. *Plant Physiol.* 163, 815–829.
- Marie, D., Simon, N., Vaulot, D., 2005. Phytoplankton Cell Counting by Flow Cytometry. In: *Algal Culturing Techniques*. 2005. Elsevier, Oxford, pp. 1–17.
- Medeiros, C., Kjerfve, B., 1988. Tidal characteristics of the strait of Magellan. *Cont. Shelf Res.* 8, 947–960.
- Menden-Deuer, S., Lessard, E.J., 2000. Carbon to volume relationships for dinoflagellates, diatoms and other protist plankton. *Limnol. Oceanogr.* 45, 569–579.
- Mitchell, B.G., 1990. Algorithms for determining the absorption coefficient for aquatic particulates using the quantitative filter technique. *Ocean optics* 10, Proc. SPIE 1302, 137–148.
- Mitchell, B.G., Kahru, M., Wieland, J., Stramska, M., 2002. Determination of spectral absorption coefficients of particles, dissolved material and phytoplankton for discrete water samples. In: Mueller J.L., Fargion G.S., McClain R. (eds) *Ocean Optics protocols for Satellite Ocean Color Sensor Validation, Revision 4, Volume IV: Inherent Optical Properties: Instruments, Characterizations, Field Measurements and Data Analysis Protocols*. NASA/TM-2003-211621, NASA Goddard Space Flight Center, Greenbelt, MD. (Chapter 4), 39–60.
- Palma, E.D., Matano, R.P., 2012. A numerical study of the Magellan plume. *J. Geophys. Res.* 117, C05041. <http://dx.doi.org/10.1029/2011JC007750>.
- Panella, S., Michelato, A., Perdicaro, R., Magazzu, G., Decembrini, F., Scarazzato, P., 1991. A preliminary contribution to the understanding of the hydrological characteristics of the Strait of Magellan: austral spring 1989. *Boll. Oceanol. Teor. Appl.* 9, 106–126.
- Perez-Cenci, M., Caló, G.F., Silva, R.I., Negri, R.M., Salerno, G.L., 2014. The first molecular characterization of Picocyanobacteria from the Argentine Sea. *J. Mar. Biol.* 8. <http://dx.doi.org/10.1155/2014/237628> (ID 237628).
- Pittera, J., Humily, F., Thorel, M., Grulois, D., Gaczarek, L., Six, C., 2014. Connecting thermal physiology and latitudinal niche partitioning in marine *Synechococcus*. *ISME J.* 8, 1221–1236.
- Pope, R.M., Fry, E.S., 1997. Absorption spectrum (380–700 nm) of Pure water: II. Integrating cavity measurements. *Appl. Opt.* 36, 8710–8723.
- Putland, J.N., 2000. Microzooplankton Herbivory and Bacterivory in Newfoundland coastal Waters during spring, summer and winter. *J. Plankton Res.* 22, 253–277.
- Ruddorf, N.M., Frouin, R., Kappel, M., Goyens, C., Meriaux, X., Schieber, B., Mitchell, B.G., 2014. Ocean-color radiometry across the southern Atlantic and South-eastern Pacific: accuracy and remote sensing implications. *Rem. Sens. Environ.* 149, 13–32.
- Saggiomo, V., Goffart, A., Carrada, G.C., Hecq, J.H., 1994. Spatial patterns of Phytoplankton pigments and primary production in a semi-enclosed Periarctic ecosystem: the Strait of Magellan. *J. Mar. Sys.* 5, 119–142.
- Saggiomo, V., Santarpia, I., Saggiomo, M., Margiotta, F., Mangoni, O., 2011. Primary production process and photosynthetic performance of a unique Periarctic ecosystem: the Strait of Magellan. *Polar Biol.* 34, 1255–1267.
- Sathyendranath, S., Platt, T., 1988. The spectral irradiance field at the surface and in the interior of the ocean: a model for applications in oceanography and remote sensing. *J. Geophys. Res.* 93, 9270–9280.
- Sathyendranath, S., Stuart, V., Nair, A., Oka, K., Nakane, T., Bouman, H., Forget, M.H., Maass, H., Platt, T., 2009. Carbon-to-chlorophyll ratio and growth rate of phytoplankton at the sea. *Mar. Ecol. Prog. Ser.* 383, 73–84.
- Scanlan, D.J., Ostrowski, M., Mazard, S., Dufresne, A., Gaczarek, L., Hess, W.R., Post, A.F., Hagemann, M., Paulsen, I., Partensky, F., 2009. Ecological genomics of marine picocyanobacteria. *Microbiol. Mol. Biol. Rev.* 73, 249–299, doi:10.1128/MMBR.00035-08.
- Sieburth, J.M., Smetacek, V., Lenz, J., 1978. Pelagic ecosystem structure: heterotrophic compartments of the plankton and their relationship to plankton size fractions. *Limnol. Oceanogr.* 23, 1256–1263.
- Silva, R., Negri, R., Lutz, V., 2009. Summer succession of ultraphytoplankton at the EPEA coastal station (Northern Argentina). *J. Plankton Res.* 31, 447–458.
- Uitz, J., Claustre, H., Morel, A., Hooker, S.B., 2006. Vertical distribution of phytoplankton communities in open ocean: an assessment based on surface chlorophyll. *J. Geophys. Res.* 111, C08005. <http://dx.doi.org/10.1029/2005JC003207>.
- Uribe, J.C., Ruiz, M., 2001. Gymnodinium brown tide in the Magellanic fjords, Southern Chile. *Revista de Biología Marina y Oceanografía* 36, 155–164.
- Utermöhl, H., 1958. Zur Vervollkommnung Der Quantitativen phytoplanktonmethodik. *Mitt. Int. Ver. Theor. Angew. Limnol.* 9, 1–38.
- Valle-Levinson, A., Blanco, J.L., Frangópulos, M., 2006. Hydrography and frontogenesis in a glacial fjord off the strait of Magellan. *Ocean Dynam.* 56, 217–227.
- Van Heukelem, L., Thomas, C.S., 2001. Computer-assisted high-performance liquid chromatography method development with applications to the isolation and analysis of phytoplankton pigments. *J. Chromatogr. A* 910, 31–49.
- Vanucci, S., Mangoni, O., 1999. Pico- and Nanophytoplankton Assemblages in a subantarctic ecosystem: the Strait of Magellan. *Bot. Mar.* 42, 563–572.
- Vezina, S., Vincent, W.F., 1996. Arctic cyanobacteria and limnological properties of their environment: Bylot Island, Northwest Territories, Canada (73°N, 80°W). *Polar Biol.* 17, 523–534.
- Waterbury, J. B., Watson, S.W., Valois, F.W., Franks, D.G., 1986. Biological and ecological characterization of the marine unicellular cyanobacterium *Synechococcus*. In: *Photosynthetic picoplankton* Platt T, Li WKW (eds). *Can. Bull. Fish. Aquat. Sci.* 214, 71–120.
- Wilmotte, A., Demonceau, C., Goffart, A., Hecq, J.H., Demoulin, V., Crossley, A.C., 2002. Molecular and pigment studies of the Picophytoplankton in a region of the southern ocean (42–54°S, 141–144°E) in March 1998. *Deep-SEA Res. II* 49, 3351–3363.
- Wright, S.W., Jeffrey, S.W., Mantoura, R.F.C., Llewellyn, C.A., Bjornland, T., Repeta, D., Welschmeyer, N., 1991. Improved HPLC method for the analysis of chlorophylls and carotenoids from marine phytoplankton. *Mar. Ecol. Prog. Ser.* 77, 183–196.
- Zingone, A., Sarno, D., Siano, R., Marino, D., 2011. The importance and distinctiveness of small-sized phytoplankton in the Magellan Straits. *Polar Biol.*, doi:10-1007/s00300-010-0937-2
- Zwirgmaier, K., Jardillier, L., Ostrowski, M., Mazard, S., Gaczarek, L., Vaulot, D., Not, F., Massana, R., Ulloa, O., Scanlan, D.J., 2008. Global Phylogeography of marine *Synechococcus* and *Prochlorococcus* reveals a distinct partitioning of lineages among oceanic biomes. *Environ. Microbiol.* 10, 147–161.